Published in final edited form as:
Hippocampus. 2012 January ; 22(1): 17–28. doi:10.1002/hipo.20859.

Synaptic loss and retention of different classic cadherins with LTP-associated synaptic structural remodeling *in vivo*

George W. Huntley[1,*], **Alice M. Elste**[1], **Shekhar B. Patil**[1], **Ozlem Bozdagi**[1], **Deanna L. Benson**[1], and **Oswald Steward**[2]

[1] Fishberg Department of Neuroscience and the Friedman Brain Institute, Box 1065, The Mount Sinai School of Medicine, 1425 Madison Avenue, New York, NY 10029

[2] Departments of Anatomy and Neurobiology, Neurobiology and Behavior, and Neurosurgery, Reeve-Irvine Research Center, University of California at Irvine College of Medicine, Irvine, CA 92697-4292

Abstract

Cadherins are synaptic cell adhesion molecules that contribute to persistently enhanced synaptic strength characteristic of long-term potentiation (LTP). What is relatively unexplored is how synaptic activity of the kind that induces LTP-associated remodeling of synapse structure affects localization of cadherins, particularly in mature animals *in vivo*, details which could offer insight into how different cadherins contribute to synaptic plasticity. Here, we use a well-described *in vivo* LTP induction protocol that produces robust synaptic morphological remodeling in dentate gyrus of adult rats in combination with confocal and immunogold electron microscopy to localize cadherin-8 and N-cadherin at remodeled synapses. We find that the density and size of cadherin-8 puncta are significantly diminished in the potentiated middle molecular layer (MML) while concurrently, N-cadherin remains tightly clustered at remodeled synapses. These changes are specific to the potentiated MML, and occur without any change in density or size of synaptophysin puncta. Thus, the loss of cadherin-8 probably represents selective removal from synapses rather than overall loss of synaptic junctions. Together, these findings suggest that activity-regulated loss and retention of different synaptic cadherins could contribute to dual demands of both flexibility and stability in synapse structure that may be important for synaptic morphological remodeling that accompanies long-lasting plasticity.

Keywords

long-term potentiation; dentate gyrus; cell adhesion molecules; synaptic plasticity; spines

Introduction

Virtually every synapse in the CNS exhibits some form of synaptic plasticity. In hippocampus, long-term potentiation (LTP) is a predominant form that is a leading cellular model of how new experiences are learned and stored within cortical circuits for recall (Whitlock et al., 2006). Each of the subfields of the hippocampus exhibits LTP, and while details differ among them, there is a general consensus that persistent changes in synaptic strength reflect posttranslational modifications and trafficking of synaptic proteins that are coordinated with morphological changes in synapse structure (Malenka and Nicoll, 1999;

[*]Correspondence to: Dr. G.W. Huntley, Fishberg Department of Neuroscience, Box 1065, The Mount Sinai School of Medicine, 1425 Madison Avenue, New York, NY 10029-6574, Phone: (212) 659-5979, Fax: (212) 996-9785, george.huntley@mssm.edu.

Yuste and Bonhoeffer, 2001). An unresolved question is how structural molecules of the synapse cell adhesion molecules respond to changes in synaptic input to enable overt restructuring of synaptic contacts, particularly at mature synapses *in vivo.*

The classic cadherins ("cadherins") are a family of cell adhesion molecules found at CNS synapses (Benson and Tanaka, 1998; Bozdagi et al., 2000; Brock et al., 2004; Elste and Benson, 2006; Fannon and Colman, 1996; Gil et al., 2002; Huntley and Benson, 1999; Jontes et al., 2004; Miskevich et al., 1998; Tang et al., 1998; Yamagata et al., 1995). These molecules are calcium-dependent, mostly homophillically-binding, single-pass transmembrane proteins that are linked via the catenin proteins to the actin cytoskeleton. Intracellularly, cadherins and their catenin binding partners interact with a number of proteins that control their adhesive properties or activate downstream signaling cascades, and include PDZ-domain-containing proteins, phosphatases, kinases, and F-actin-associated proteins (Arikkath and Reichardt, 2008). Cadherins have been implicated in maintenance of LTP in acute hippocampal slices on the basis of bath-applied blocking reagents (Bozdagi et al., 2000; Tang et al., 1998) or genetic elimination (Manabe et al., 2000). These approaches indicate that cadherins contribute to mechanisms that regulate strength of synaptic activity. What is less clear, however, is the converse how does synaptic activity of the kind that leads to structural remodeling affect cadherin localization and/or function? responses that may be important for inferring ways in which cadherins contribute to synaptic plasticity. For example, in cultured hippocampal neurons and/or acute slices, strong synaptic activity stabilizes surface N-cadherin (Tai et al., 2007), promotes its synthesis and dimerization (Bozdagi et al., 2000; Tanaka et al., 2000), and increases its association with β-catenin (Murase et al., 2002), all indices of enhanced N-cadherin adhesive strength. In contrast, E-cadherin is rapidly lost from dorsal horn synapses in neuropathic pain models associated with synaptic circuit remodeling (Brock et al., 2004; Seto et al., 1997). Although speculative, the loss of this cadherin may facilitate such synaptic reorganization, akin to the surface removal of the cell adhesion molecule apCAM in Aplysia, which facilitates growth of new synaptic connections during long-lasting forms of plasticity (Mayford et al., 1992).

Here, we use a well-characterized protocol for LTP-associated synaptic remodeling in adult dentate gyrus *in vivo* and take an anatomical approach to investigate whether and how different synaptic cadherins respond under structural plasticity-inducing stimulation conditions. In this *in vivo* LTP model, repetitive tetanic stimulation of medial perforant path fibers leads to elaboration of dendritic spines in the middle molecular layer such that they enwrap their presynaptic terminals (forming so-called "concave synapses"), producing synapses with longer, more extensive zones of synaptic membrane apposition (Desmond and Levy, 1986; Desmond and Levy, 1988; Geinisman et al., 1991; Popov et al., 2004; Weeks et al., 1999; Weeks et al., 2000; Weeks et al., 2001). While the precise functional significance of such overt synaptic structural remodeling is uncertain, and not the focus here, the observation that such morphological spine elaborations occur strictly with LTP rather than merely reflecting the high-frequency tetanic stimuli typically used to generate LTP suggests an important contribution to the induction and/or maintenance of persistent changes in synaptic strength (Weeks et al., 2003). One important open question is what are the molecular mechanisms that ensure the dual demands of both stability of apposed pre- to postsynaptic membranes and flexibility in such appositions to allow for morphological remodeling? In epithelia, a similar conundrum may be solved by mechanisms that regulate stable and mobile cadherin-based adhesive contacts (Cavey et al., 2008). Here, we find that cadherin-8 is significantly diminished at remodeled synapses selectively in the potentiated MML while simultaneously N-cadherin remains tightly clustered at such synapses, suggesting a basis for both stability and flexibility of synaptic structure. While there are multiple classic cadherins expressed in hippocampus and connectionally-related structures,

we focus on cadherin-8 and N-cadherin because they are two of the most prominently expressed in these circuits (Bekirov et al., 2002; Korematsu and Redies, 1997).

Materials and Methods

Animals

Experiments were conducted on a total of 12 adult male Sprague-Dawley rats (200–400 gms). Electrophysiological studies were conducted at UC Irvine. Additional animals were subjected to electrophysiological experiments at Mount Sinai using similar procedures to those at UC Irvine. The brains of all animals, as well as those from naïve (unstimulated) animals, were subsequently processed for immunolabeling and analyzed by confocal or electron microscopy at Mount Sinai. All procedures were approved by the Institutional Animal Care and Use Committees of UC Irvine and Mount Sinai, and followed guidelines established by the National Institutes of Health.

Electrophysiology

Procedures to induce LTP of medial perforant path input to the dentate gyrus *in vivo* have been detailed previously (Levy and Steward, 1979; Steward et al., 1990; Steward et al., 1998). Briefly, rats were anesthetized with urethane (1.5 g/kg i.p.) and placed in a stereotaxic instrument. A monopolar tungsten stimulating electrode was positioned stereotactically (4.0 mm lateral to the midline; 1.0 mm anterior to the transverse sinus) in order to selectively activate the afferent projections from the medial entorhinal cortex (EC) to the middle molecular layer (MML) of the ipsilateral dentate gyrus (DG). The depth of the stimulating electrode was adjusted so as to obtain a maximal evoked response in the DG at minimal stimulus intensity. A recording electrode (a glass micropipette filled with 0.9% saline) was positioned in the cell layer of the ipsilateral DG (1.5–2.0 mm lateral to the midline; 3.5 mm posterior to bregma) based on evoked responses generated by EC stimulation. Stimulus intensity was set so as to evoke an 1–3 mV population spike. Baseline responses were collected for 10 min with single test pulses delivered at a rate of 1/10 sec. Thereafter, LTP of synapses in the ipsilateral MML was induced by high-frequency stimulation (HFS; each train consists of 8 pulses at 400 Hz) delivered at a rate of 1 train/10 sec for 0.25, 1 or 2 hrs. Control rats received low frequency stimulation (0.8 pulses/sec, hereafter referred to as “controls”) over comparable periods that delivers the same number and intensity of stimuli but does not cause LTP (Moga et al., 2004; Steward and Halpain, 1999). At the end of the period of electrical stimulation, test responses were delivered in order to determine the extent of the synaptic potentiation that had been induced.

Primary antibodies and immunofluorescence

Animals were perfused through the ascending aorta with cold 1% paraformaldehyde followed by cold 4% paraformaldehyde in 0.1 M phosphate buffer (PB) for 10 min. Brains were removed, postfixed for 4 hrs, and sectioned serially in the frontal plane through the dorsal hippocampus bilaterally on a vibratome. Methods of antigen retrieval, immunofluorescent labeling, confocal microscopy and analysis were according to our previous descriptions (Bozdagi et al., 2000; Brock et al., 2004; Gil et al., 2002). Briefly, sections were subjected to a mild enzymatic digestion protocol (pepsin A, 0.1 mg/ml in 0.2 N HCl) to enhance labeling of synaptically-enriched proteins (Fukaya and Watanabe, 2000). After washing, sections were then incubated overnight in one or more of the following: goat polyclonal anti-cadherin-8 antiserum (C-18, 1:100, Santa Cruz Biochemical, Santa Cruz, CA, catalog #sc-6461); mouse monoclonal N-cadherin antibody (1:400; BD Biosciences, San Jose, CA, clone 32, catalog #610921); mouse monoclonal anti-synaptophysin antibody (1:200, Sigma-Aldrich, Saint Louis, MO, clone SVP-38, catalog #S5768), or a cocktail of guinea-pig polyclonal vesicular glutamate transporter 1 and 2 antisera (1:20,000 and 1:1000,

respectively, Millipore Bioscience Research Reagents, Temecula, CA, catalog #s AB5909 and AB5907). Primary antibody binding was subsequently visualized by incubating sections in species-appropriate, Alexa fluorophore-conjugated secondary antibodies (Jackson ImmunoResearch, West Grove, PA) for 2 hours at room temperature. Sections were then coverslipped for analysis.

Cadherin antibody characterization and controls for light microscopy

The cadherin-8 antiserum was raised against an 18 amino acid sequence of the C-terminus that mapped to a region spanning amino acids 700–750 of human cadherin-8. We verified specificity by immunoblotting lysates prepared from L-cells transfected with full-length rat cadherin-8 (gift of Dr. S. T. Suzuki) or lysates prepared from adult rat whole hippocampus (Fig. 1). In both cases, a single band of ~130 kd was observed, which is similar to the reported size of cadherin-8 when expressed in L-cells and in whole rat brain lysates (Kido et al., 1998), or in lysates prepared from mouse spinal cord (Suzuki et al., 2007). The N-cadherin antibody was raised against a portion of the C-terminus (aa 735–883) and its specificity has been verified previously (Brock et al., 2004). In brief, it recognizes L-cells expressing N-cadherin but not those expressing E-cadherin. Additionally, immunoblot analysis of hippocampal or spinal cord lysates shows a single band of the appropriate (~125 kd) molecular mass, and no labeling is found in postsynaptic density fractions isolated from N-cadherin conditional knockout mice (Bozdagi et al., 2010). Controls for non-specific binding of the secondary antibodies included processing sections immunofluorescently as described except for omitting the primary antibodies. No specific labeling was observed under these conditions.

Confocal microscopy and analysis

Immunofluorescent localization of cadherins and the other synaptic markers in the dentate gyrus was analyzed by confocal microscopy using a 100X, 1.4 N.A. oil-immersion objective (Zeiss LSM 510, Thornwood, NY) as described in detail previously (Brock et al., 2004; Huntley and Benson, 1999). For qualitative assessment of codistribution of cadherin-8 and vGlut labeling, single optical sections through the MML were acquired from naïve (unstimulated) rats from two channels simultaneously with a dichroic beam splitter. These images were compared with data acquired sequentially by using one laser line to ensure emission spectra were clearly separated. For quantitative analysis, high-resolution, single optical images of cadherin-8, N-cadherin or synaptophysin labeling were acquired from the inner molecular layer (IML), the MML and the outer molecular layer (OML) of the ipsilateral (HFS or control-stimulated) dentate gyrus (suprapyramidal blade). Mindful of the possibility of uneven or differential antibody penetration into the depth of the tissue, pilot scans of each set of sections were done to determine the depth (z-plane) of antibody penetration; thereafter, images were always acquired from surface regions (~1–6 μm) in which label was consistently present across sections and conditions. Qualitative, low-power inspection of cadherin or synaptophysin immunolabeled sections revealed no obvious differences in labeling patterns across the range of stimulation times used, thus data were combined. For comparisons between HFS and control stimulation conditions, brightness and contrast were optimized for each sublayer of the control stimulation sections and then held constant during acquistion of images of the corresponding sublayer in HFS sections. Images from a minimum of three microscope fields were acquired from each sublayer from 3–5 sections per rat. The imaging fields were determined pseudo-randomly for each section by qualitatively dividing the suprapyramidal blade into lateral, middle and medial thirds, and acquiring one image per each of these divisions. Sublayers were determined by dividing the total distance of the molecular layer into three zones of 25% (IML), 40% (MML) and 35% (OML) of the total distance. A thresholding function to capture labeled puncta was then applied to deconvolved images using Metamorph software (Universal Imaging Corp.,

Downingtown, PA), as described (Bozdagi et al., 2000) and used to determine puncta number per unit area and cross-sectional area. Such values for each sublayer were then averaged per animal. Data are expressed as mean values across animals + SEM, and were compared using unpaired t-tests with a Bonferroni correction for multiple comparisons. A minimum criterion of $p<0.05$ (following correction) was considered a statistically significant difference.

Post-embedding immunoelectron microscopy

Animals (receiving 1 or 2 hr HFS) were perfused with a mixture of 2% paraformaldehyde and 2% glutaraldehyde in 0.1 M PB and processed by a freeze-substitution, low-temperature Lowicryl embedding protocol (Chaudhry et al., 1995; van Lookeren Campagne et al., 1991) for postembedding immunogold localization of synaptic N-cadherin as detailed previously (Elste and Benson, 2006). Ultra-thin sections through the MML were cut on a Reichert-Jung ultramicrotome and mounted on formvar-coated nickel grids. Sections were then exposed overnight to rabbit polyclonal anti-N-cadherin antiserum (Tanaka et al., 2000) (gift from Dr. David Colman, Montreal Neurological Institute). Primary antibody binding was visualized by goat anti-rabbit IgG secondary antibodies conjugated to10 nm gold (BB International, Cardiff, UK). Grids were then rinsed and counterstained with lead citrate and uranyl acetate. Grids were examined on a Jeol 1200EX electron microscope and digital images were taken with an Advantage CCD camera (Advanced Microscopy Techniques, Danvers, MA). The generation and specificity of the N-cadherin antiserum has been described (Tanaka et al., 2000) and controls to verify specificity under identical conditions have been detailed previously (Elste and Benson, 2006). Briefly, the affinity-purified antiserum was generated against the entire C-terminus of mouse N-cadherin fused to glutathione transferase. Controls included omitting the primary antiserum; replacing the primary antiserum with normal rabbit IgG at the same protein concentration; preadsorption with the glutathione S-transferase (GST)-N-cadherin intracellular domain fusion protein; and preadsorption of the primary antiserum with GST alone. Only an occasional gold particle was detected under the first three control conditions and these appeared randomly distributed. Results under the last control condition appeared identical to sections processed with the N-cadherin antiserum alone. Adjustments to the images, including size, brightness, and contrast were carried out using Adobe PhotoShop CS4 (Adobe Systems, San Jose, CA). Final figure layout and additional graphics were completed using Adobe InDesign CS4.

Results

Cadherin-8 is synaptically localized in adult rat dentate gyrus

We first investigated whether cadherin-8 localizes to synaptic junctions in adult dentate gyrus. Aldehyde-fixed tissue sections were immunofluorescently labeled for cadherin-8 and for one of several markers of presynaptic terminals, including synaptophysin (Navone et al., 1986) and vesicular glutamate transporters 1 and 2 (vGluts) (Fremeau et al., 2004; Kaneko et al., 2002). Confocal microscopy showed that cadherin-8 immunolabeling within the dentate gyrus molecular layer was punctate (Fig. 2A); the majority of such puncta codistributed with immunolabeling for synaptophysin or vGluts (Fig. 2B, C). The pattern of codistribution was one with a central area of overlap (yellow pixels) offet by single labeling for the presynaptic marker synaptophysin or vGluts (inset, Fig. 2C), which is identical to previous descriptions of synaptic localization of cadherin-8 and other cadherins by similar methods (Huntley, 2002). There were, additionally, some cadherin-8 puncta that did not codistribute with these presynaptic markers. It is possible that such non-synaptic puncta represent cadherin-8 localization at adhesive puncta adherens (Bahjaoui-Bouhaddi et al., 1997; Brock et al., 2004; Fannon et al., 1995; Takeichi, 1990). Overall, the data indicate that

cadherin-8 is localized mostly to synaptic or perisynaptic regions within the adult dentate gyrus molecular layer.

Altered pattern of cadherin-8 localization in MML following HFS

We next investigated whether cadherin-8 localization changes in association with overt structural synaptic remodeling that accompanies dentate gyrus LTP *in vivo*. Here, we applied to anesthetized adult rats HFS of the afferent projections from medial EC to the ipsilateral DG that is well-known to produce morphological remodeling of dendritic spines (concave synapses) within the middle molecular layer (MML) (Desmond and Levy, 1986; Geinisman et al., 1991; Weeks et al., 2003; Weeks et al., 2000), the main site of termination of fibers of the medial perforant path (Steward, 1976). A representative example of such HFS-induced LTP is shown in Fig. 3. We verified by electron microscopy that HFS resulted in changes in synaptic morphology as characterized previously. Figure 4 shows that, as expected, the neuropil of the potentiated MML was filled with synaptic profiles in which postsynaptic spines (arrows, Fig. 4A) enwrapped the presynaptic terminals (asterisks, Fig. 4A), in some cases encircling the presynaptic terminal so completely as to form a seemingly novel membrane apposition at the point of contact (arrowheads, Fig. 4A). In contrast, synaptic profiles in the MML of control tissue were either roughly linear or mildly concave-shaped (arrows, Fig. 4B). We next immunolabeled control and HFS sections through dentate gyrus and analyzed the tissue by confocal microscopy. In control sections, cadherin-8 immunolabeling was relatively homogeneous across the molecular layer (Fig. 5A, C). In contrast, in HFS sections, cadherin-8 immunolabeling was greatly diminished in a restricted band corresponding to the MML (Fig. 5B, D). Quantitative analysis of cadherin-8 immunoreactive puncta within the MML of HFS and control-stimulation tissue revealed that such diminished labeling was a reflection of significant decreases in both number of puncta (Fig. 6A) and size of those that remain (Fig. 6B). To verify the specificity of such effects in relationship to the location of the potentiated and morphologically remodeled synapses, we examined cadherin-8 immunolabeling in the layers that flank the stimulated MML (inner and outer molecular layers) in comparison with that in the corresponding layers of control sections. Figure 6 shows that there were no differences between HFS and control sections in the numbers (Fig. 6A) or the sizes (Fig. 6B) of cadherin-8 puncta in either of these two flanking, unstimulated layers. These data indicate that such changes in cadherin-8 localization are specific to the layer undergoing synaptic potentiation and morphological remodeling. We attempted to localize cadherin-8 ultrastructurally by postembedding immunogold in order to determine if, at the cadherin-8 puncta that remained, there were changes in fine localization in relationship to the altered synaptic morphology, but the cadherin-8 antiserum was not compatible with these techniques.

Synaptophysin labeling unchanged by HFS

The striking reduction in cadherin-8 immunolabeling specifically from synapses in the MML from HFS rats suggests either that numbers of synaptic junctions themselves are decreased or that cadherin-8 protein is selectively lost from otherwise stable, but remodeled synaptic junctions. To test this, we immunolabeled HFS and control sections for synaptophysin, a presynaptic vesicle glycoprotein. In hippocampus and elsewhere, immunolabeled synaptophysin clusters have been used previously to estimate density of presynaptic boutons (Calhoun et al., 1996; Smith et al., 2000). Figure 7 shows no obvious changes in the pattern of synaptophysin labeling in the MML of HFS rats in comparison with that in the MML of control tissue (Fig. 7A, B). This qualitative impression was verified quantitatively; there were no differences between control and HFS conditions in density (Fig. 7C) or sizes (Fig. 7D) of synaptophysin puncta in the MML or in flanking layers (IML and OML). These data suggest that cadherin-8 is selectively reduced at synapses rather than reflecting an overall loss of the synaptic junctions themselves. This is consistent with

previous ultrastructural studies showing no overall decrease in synapse number within the MML following LTP *in vivo* (Desmond and Levy, 1990; Geinisman et al., 1991; Weeks et al., 2000).

N-cadherin is retained at synaptic membranes of remodeled synaptic junctions

Finally, we asked whether other cadherins are affected similarly by such HFS-related morphological changes in synaptic structure. Control and HFS sections were immunolabeled for N-cadherin and analyzed by confocal microscopy. Both qualitative (Fig. 8A, B) and quantitative (Fig. 8C) comparisons of N-cadherin labeling within the MML showed that there were no differences between HFS and control sections in numbers of immunoreactive puncta. This result implies that N-cadherin remains at morphologically remodeled synapses within the potentiatied MML, which was verified by immunogold electronmicroscopy. Within the neuropil of the MML of HFS rats, N-cadherin gold particles were clustered, usually at the edges of pre- and postsynaptic densities of asymmetric synapses (dotted arrow, Fig. 8D) in which the postsynaptic elements exhibit the typical LTP-associated curvature (solid arrows, Fig. 8D). Such localization is similar to that observed in the MML of control sections, where synaptic curvature is much less pronounced (dotted arrow, Fig. 8E).

Discussion

We describe here differential effects on localization of cadherin-8 and N-cadherin, two structurally and functionally different members of the cadherin family of synaptic adhesion proteins, in adult rat dentate gyrus in response to a well-described *in vivo* HFS protocol that produces robust synaptic morphological remodeling and LTP. Such remodeling is characterized principally by a dramatic increase in synaptic curvature (postsynaptically "concave" synapses) restricted to the MML (Desmond and Levy, 1986; Geinisman et al., 1991; Weeks et al., 2003; Weeks et al., 2000). Our data demonstrate that both cadherin-8 and N-cadherin are enriched at synapses in dentate gyrus. However, following HFS, the density and sizes of cadherin-8 puncta are significantly reduced at synaptic or peri-synaptic regions within the potentiated MML. Such changes in density of immunolabeled synaptic puncta are lamina specific, as density and size of cadherin-8 puncta in flanking (unpotentiated) laminae are unchanged. Such loss of cadherin-8 labeling likely reflects reduction or removal of the protein from synapses undergoing remodeling, rather than overall loss of synaptic junctions per se, since density and sizes of synaptophysin-labeled boutons are unchanged by HFS. In contrast to significantly diminished levels of synaptic cadherin-8, localization and levels of N-cadherin are unchanged at remodeled synapses following HFS. This indicates that cadherin-8 is removed or reduced selectively. Taken together, the reduction of cadherin-8 and the retention of N-cadherin during HFS-induced remodeling of the synaptic neuropil suggests distinct roles for each of these cadherins in synaptic function and plasticity. The loss of cadherin-8 may enable a flexibility in membrane-membrane apposition allowing for dynamic changes in morphology of synapse-bearing profiles such as spines and boutons, while the retention of N-cadherin at synaptic membranes within those profiles may coordinate and preserve the strict apposition of pre-to-postsynaptic densities and associated proteins necessary for synaptic signaling.

Mechanisms of loss and retention of different cadherins at potentiated synapses

Differences between cadherin-8, a type II classic cadherin, and N-cadherin, a type I classic cadherin, in their anchoring at the synaptic membrane and the ways in which synaptic activity regulates their function and/or positioning may account for the loss and retention of these cadherins, respectively, with HFS. Proteomic analysis suggests that N-cadherin is a component of a large, NMDA receptor-enriched complex of synaptic proteins and while it is

unknown if cadherin-8 is similarly included, other type II cadherins are not included (Husi et al., 2000). Thus, N-cadherin may be inherently more stable at the synapse by virtue of the myriad of protein-protein intereractions with which it engages (Arikkath and Reichardt, 2008). Additionally, strong synaptic activity of the kind that induces LTP may differentially drive changes in the molecular configuration of these cadherins, the level of cadherins present at the synapse, and their association with actin-binding or scaffolding proteins. For example, strong depolarization of cultured hippocampal neurons or LTP-inducing stimuli applied to hippocampal slices promote N-cadherin cis-strand dimerization and resistence to extracellular proteolytic degradation (Bozdagi et al., 2000; Tanaka et al., 2000), two indices of strong adhesion (Brieher et al., 1996; Tamura et al., 1998). Moreover, NMDA receptor activity stabilizes surface N-cadherin by diminishing the rate of basal endocytosis (Tai et al., 2007), and upon late-phase LTP, additional N-cadherin is synthesized and recruited to synaptic sites (Bozdagi et al., 2000). Together, these data suggest that N-cadherin mediated adhesive force across the synapse is strengthened during LTP. This idea is supported further by studies that show that strong synaptic activity drives β-catenin, which is necessary for anchoring cadherins to the actin cytoskeleton, from the dendritic shaft into spines, where its association with cadherins is enhanced (Murase et al., 2002). Although immunoprecipitation studies indicate that cadherin-8 also associates with β-catenin in dentate gyrus (Bekirov et al., 2008), the observation here that cadherin-8 is significantly diminished at potentiated synapses suggests that it is not the beneficiary of enhanced β-catenin linkage to the cytoskeleton under these conditions. Additionally, the postsynaptic scaffolding protein AKAP79/150 (A-kinase-anchoring protein) is upregulated in dentate gyrus with *in vivo* LTP (Genin et al., 2003), and recent studies indicate that AKAP79/150 binds to N-cadherin directly (Gorski et al., 2005), suggesting a further role in anchoring synaptic N-cadherin during LTP.

In contrast to activity-dependent effects on N-cadherin, cadherin-8 does not undergo such dimerization in response to strong synaptic depolarization (Tanaka et al., 2000), leaving cadherin-8 vulnerable to HFS-activated proteolytic degradation (Kido et al., 1998). Recent studies indicate that matrix metalloproteinase (MMP)-mediated perisynaptic proteolysis is induced rapidly in hippocampus by LTP-inducing stimuli (Bozdagi et al., 2007; Nagy et al., 2007), and is required for LTP-associated dendritic spine morphological remodeling (Wang et al., 2008). Although it is not known if cadherin-8 is an endogenous substrate for MMP-mediated proteolysis, it has been demonstrated previously in cultured hippocampal neurons and other cell types that MMPs can cleave the ectodomains of some type I cadherins (Marambaud et al., 2002; Monea et al., 2006), the C-terminal fragments of which are then degraded further by a proteosome pathway (Ito et al., 1999). Additionally, in response to LTP-inducing stimulation, MMP-mediated shedding of ICAM5 (also called telencephalin), an adhesion protein of the Ig-superfamily, has been demonstrated recently (Conant et al., 2010; Tian et al., 2007). As NMDA receptor activity is required for the molecular reconfiguration and surface stabilization of N-cadherin, and for the activation of MMP proteolysis (Nagy et al., 2006; Tai et al., 2007; Tanaka et al., 2000), our data, together with previous studies, suggest a speculative model whereby NMDA receptor activity during LTP induction triggers unknown intracellular pathways that serve to stabilize, strengthen and protect N-cadherin mediated adhesion from proteolytic degradation, while simultaneously activating perisynaptic, extracellular proteolysis that could cleave, and ultimately dismantle, cadherin-8. It is important to emphasize, however, that on the basis of the experiments presented here, we cannot distinguish whether the changes in cadherin-8 reflect the prolonged HFS per se, or the LTP that results from it. It is clear though, that the two cadherins respond differently to strong and prolonged synaptic activation.

The functional significance of HFS-associated loss and retention of different synaptic cadherins is speculative. Cell aggregation assays suggest that cadherin-8 adhesion is

inherently weaker than N-cadherin adhesion (Kido et al., 1998), which may reflect the significant differences in the structure of their adhesive interfaces (Patel et al., 2006). During hippocampal circuit development, cadherin-8 and N-cadherin contribute to different aspects of pre- and postsynaptic development and targeting (Bekirov et al., 2008), indicating that despite overall similarities in structure, they do not perform redundant functions. It is possible that at the synapse, cadherin-8 function in adhesion per se is minimal; rather, it may function as a co-receptor with other cell surface adhesion or extracellular matrix (ECM) proteins (Balsamo and Lilien, 1990; Rhee et al., 2002; Tanaka et al., 2003). For example, local regulation of ECM proteins occurs with LTP (Dityatev and Schachner, 2003), which might be necessary to facilitate local, coordinated morphological remodeling of both pre- and postsynaptic elements and the surrounding glia that contact them (Haber et al., 2006). In other cell types, integrins, which are receptors for matrix proteins, can interact directly and indirectly with cadherins (Juliano, 2002). Thus, diminished labeling for cadherin-8 might reflect local remodeling of an integrated network of ECM molecules and the cell surface proteins with which they interact to facilitate subtle morphological reorganization. In contrast, the prevailing evidence discussed above indicates that N-cadherin adhesion is enhanced during LTP, and this may be necessary in part to maintain tight apposition of pre-to-postsynaptic membranes in the face of an enlarging synaptic surface area (Desmond and Levy, 1986; Desmond and Levy, 1988). It is also likely that N-cadherin plays a proactive role in the process of functional and structural plasticity associated with LTP, perhaps by driving morphological changes directly (Bozdagi et al., 2010; Mendez et al., 2010; Mysore et al., 2007; Okamura et al., 2004; Togashi et al., 2002; Xie et al., 2008); by regulating the trafficking and localization of AMPA-type or other glutamate receptor subunits (Coussen et al., 2002; Nuriya and Huganir, 2006; Saglietti et al., 2007; Silverman et al., 2007); by affecting presynaptic vesicle release (Bozdagi et al., 2004; Jungling et al., 2006) or by increasing voltage-gated calcium influx (Marrs et al., 2009). Consistent with this idea, it has been shown recently that conditional deletion of N-cadherin at mature synapses impairs persistence of theta-induced LTP and LTP-associated spine enlargement at CA1 synapses (Bozdagi et al., 2010), as well as reduces spine stability (Mendez et al., 2010).

It is likely that cadherin-8 and N-cadherin are co-expressed within the same pre-and postsynaptic population of neurons, as combinatorial expression of multiple cadherins by single neurons is well-described (Miskevich et al., 1998; Wöhrn et al., 1999), and both cadherin-8 and N-cadherin mRNAs are expressed by densely distributed neurons in entorhinal cortex and dentate gyrus (Bekirov et al., 2002; Korematsu and Redies, 1997; Redies and Takeichi, 1993). However, our data do not necessarily indicate that these two cadherins are expressed at the same synapses. It is conceivable that they sort to separate synapses within the MML, possibly conferring different attributes of synaptic plasticity to different synaptic populations, but future studies will be required to determine this.

Pattern of synaptic fine-localization of N-cadherin following HFS suggests remodeled, not new, synapses

There is a general consensus from several previous studies that there are no net changes in synapse number-per-neuron or neuropil density associated with LTP of the perforant path input to the MML of the dentate gyrus at times ranging from hours to weeks post-LTP induction (Geinisman et al., 1991; Geinisman et al., 1993; Geinisman et al., 1996; Popov et al., 2004; Weeks et al., 2000; Weeks et al., 2001). Such conclusions are based on unbiased stereological measures derived from serial electron micrographs, although similar conclusions have been drawn from single-ultrathin section counts as well (Desmond and Levy, 1983; Desmond and Levy, 1990). Consistent with these conclusions, we found no differences in the density or sizes of synaptophysin or N-cadherin immunoreactive puncta between HFS and control-stimulated MMLs at the 1–2 hr timepoints. Our data do not rule

out that changes in density of immunolabeled synaptic puncta could occur at later timepoints (Stewart et al., 2000), nor that other novel synaptic associations occur, such as the formation of multiple-synapse boutons (Kirov et al., 1999; Toni, 1999). Nevertheless, it has been an open question whether in mature animals, the lack of net changes in numbers of synapses with LTP reflects a static population of synapses or equal rates of synapse formation and elimination (Popov et al., 2004; Sorra and Harris, 1998). While this question was not the major focus of the current study, the fine-pattern of N-cadherin immunogold labeling at remodeled synapses may provide some insight. Ultrastructurally, the fine-localization of N-cadherin at the synaptic junction undergoes a developmentally-regulated redistribution that has been suggested to reflect the state of maturity of the synapse (Elste and Benson, 2006). At young or immature synapses, N-cadherin immunogold labeling is distributed evenly along apposed pre- and postsynaptic densities or, by peroxidase labeling, along the synaptic cleft (Yamagata et al., 1995), but at mature synaptic junctions, immunogold labeling for N-cadherin or for alpha-N-catenin is clustered, and often found at an edge or in the middle of the densities (Elste and Benson, 2006; Uchida et al., 1996). It has been proposed that such differential patterns could be used as a telltale signature of the maturational history of individual synapses (Elste and Benson, 2006). In our material, N-cadherin immunogold labeling at the remodeled synapses formed clusters, usually at the edges of the densities, which, by the criteria above, would indicate that mature, preexisting synapses underwent HFS-associated morphological remodeling rather than a *de novo* population of new synapses arising in response to stimulation.

Acknowledgments

We are grateful to Dr. Matthew Shapiro and his laboratory for supplying some tissue for this study. We also thank Dr. S.T. Suzuki for the gift of the cadherin-8 construct and Dr. Iddil Bekirov for help with characterizing the specificity of the cadherin-8 antiserum.

Grant sponsor: National Institutes of Health, U. S. Public Health Service; Grant numbers: R01MH075783, R01NS037731 and R01NS12333.

Literature Cited

Arikkath J, Reichardt LF. Cadherins and catenins at synapses: roles in synaptogenesis and synaptic plasticity. Trends Neurosci. 2008; 31:487–494. [PubMed: 18684518]

Bahjaoui-Bouhaddi M, Padilla F, Nicolet M, Cifuentes-Diaz C, Fellmann D, Mege RM. Localized deposition of M-cadherin in the glomeruli of the granular layer during the postnatal development of mouse cerebellum. J Comp Neurol. 1997; 378:180–195. [PubMed: 9120059]

Balsamo J, Lilien J. N-cadherin is stably associated with and is an acceptor for a cell surface N-acetylgalactosaminylphosphotransferase. J Biol Chem. 1990; 265:2923–2928. [PubMed: 2154466]

Bekirov IH, Nagy V, Svoronos A, Huntley GW, Benson DL. Cadherin-8 and N-cadherin differentially regulate pre- and postsynaptic development of the hippocampal mossy fiber pathway. Hippocampus. 2008; 18:349–363. [PubMed: 18064706]

Bekirov IH, Needleman LA, Zhang W, Benson DL. Identification and localization of multiple classic cadherins in developing rat limbic system. Neuroscience. 2002; 115:213–227. [PubMed: 12401335]

Benson DL, Tanaka H. N-cadherin redistribution during synaptogenesis in hippocampal neurons. J Neurosci. 1998; 18:6892–6904. [PubMed: 9712659]

Bozdagi O, Nagy V, Kwei KT, Huntley GW. In vivo roles for matrix metalloproteinase-9 in mature hippocampal synaptic physiology and plasticity. J Neurophysiol. 2007; 98:334–344. [PubMed: 17493927]

Bozdagi O, Shan W, Tanaka H, Benson DL, Huntley GW. Increasing numbers of synaptic puncta during late-phase LTP: N-cadherin is synthesized, recruited to synaptic sites, and required for potentiation. Neuron. 2000; 28:245–259. [PubMed: 11086998]

Bozdagi O, Valcin M, Poskanzer K, Tanaka H, Benson DL. Temporally distinct demands for classic cadherins in synapse formation and maturation. Mol Cell Neurosci. 2004; 27:509–521. [PubMed: 15555928]

Bozdagi O, Wang X-B, Nikitczuk JS, Anderson TR, Bloss EB, Radice GL, Zhou Q, Benson DL, Huntley GW. Persistence of coordinated LTP and dendritic spine enlargment at mature hippocampal CA1 synapses requires N-cadherin. J Neurosci. 2010 in press.

Brieher WM, Yap AS, Gumbiner BM. Lateral dimerization is required for the homophilic binding activity of C-cadherin. J Cell Biol. 1996; 135:487–496. [PubMed: 8896604]

Brock JH, Elste A, Huntley GW. Distribution and injury-induced plasticity of cadherins in relationship to identified synaptic circuitry in adult rat spinal cord. J Neurosci. 2004; 24:8806–8817. [PubMed: 15470146]

Calhoun ME, Jucker M, Martin LJ, Thinakaran G, Price DL, Mouton PR. Comparative evaluation of synaptophysin-based methods for quantification of synapses. J Neurocytol. 1996; 25:821–828. [PubMed: 9023727]

Cavey M, Rauzi M, Lenne PF, Lecuit T. A two-tiered mechanism for stabilization and immobilization of E-cadherin. Nature. 2008; 453:751–756. [PubMed: 18480755]

Chaudhry FA, Lehre KP, van Lookeren Campagne M, Ottersen OP, Danbolt NC, Storm- Mathisen JG. Glutamate transporters in glial plasma membranes: highly differentiated localizations revealed by quantitative ultrastructural immunocytochemistry. Neuron. 1995; 15:711–720. [PubMed: 7546749]

Conant K, Wang Y, Szklarczyk A, Dudak A, Mattson MP, Lim ST. Matrix metalloproteinase-dependent shedding of intercellular adhesion molecule-5 occurs with long-term potentiation. Neuroscience. 2010; 166:508–521. [PubMed: 20045450]

Coussen F, Normand E, Marchal C, Costet P, Choquet D, Lambert M, Mege RM, Mulle C. Recruitment of the kainate receptor subunit glutamate receptor 6 by cadherin/catenin complexes. J Neurosci. 2002; 22:6426–6436. [PubMed: 12151522]

Desmond NL, Levy WB. Synaptic correlates of associative potentiation/depression: an ultrastructural study in the hippocampus. Brain Res. 1983; 265:21–30. [PubMed: 6850319]

Desmond NL, Levy WB. Changes in the postsynaptic density with long-term potentiation in the dentate gyrus. J Comp Neurol. 1986; 253:476–482. [PubMed: 3025273]

Desmond NL, Levy WB. Synaptic interface surface area increases with long-term potentiation in the hippocampal dentate gyrus. Brain Res. 1988; 453:308–314. [PubMed: 3401768]

Desmond NL, Levy WB. Morphological correlates of long-term potentiation imply the modification of existing synapses, not synaptogenesis, in the hippocampal dentate gyrus. Synapse. 1990; 5:139–143. [PubMed: 2309158]

Dityatev A, Schachner M. Extracellular matrix molecules and synaptic plasticity. Nat Rev Neurosci. 2003; 4:456–468. [PubMed: 12778118]

Elste AM, Benson DL. Structural basis for developmentally regulated changes in cadherin function at synapses. J Comp Neurol. 2006; 495:324–335. [PubMed: 16440298]

Fannon AM, Colman DR. A model for central synaptic junctional complex formation based on the differential adhesive specificities of the cadherins. Neuron. 1996; 17:423–434. [PubMed: 8816706]

Fannon AM, Sherman DL, Ilyina-Gragerova G, Brophy PJ, Friedrich VL Jr, Colman DR. Novel E-cadherin-mediated adhesion in peripheral nerve: Schwann cell architecture is stabilized by autotypic adherens junctions. J Cell Biol. 1995; 129:189–202. [PubMed: 7698985]

Fremeau RT Jr, Kam K, Qureshi T, Johnson J, Copenhagen DR, Storm-Mathisen J, Chaudhry FA, Nicoll RA, Edwards RH. Vesicular glutamate transporters 1 and 2 target to functionally distinct synaptic release sites. Science. 2004; 304:1815–1819. [PubMed: 15118123]

Fukaya M, Watanabe M. Improved immunohistochemical detection of postsynaptically located PSD-95/SAP90 protein family by protease section pretreatment: a study in the adult mouse brain. J Comp Neurol. 2000; 426:572–586. [PubMed: 11027400]

Geinisman Y, de Toledo-Morrell L, Morrell F. Induction of long-term potentiation is associated with an increase in the number of axopinous synapses with segmented postsynaptic densities. Brain Res. 1991; 566:77–88. [PubMed: 1814558]

Geinisman Y, de Toledo-Morrell L, Morrell F, Heller RE, Rossi M, Parshall RF. Structural synaptic correlate of long-term potentiation: formation of axospinous synapses with multiple, completely partitioned transmission zones. Hippocampus. 1993; 3:435–445. [PubMed: 8269035]

Geinisman Y, Detoledo-Morrell L, Morrell F, Persina IS, Beatty MA. Synapse restructuring associated with the maintenance phase of hippocampal long-term potentiation. J Comp Neurol. 1996; 368:413–423. [PubMed: 8725348]

Genin A, French P, Doyere V, Davis S, Errington ML, Maroun M, Stean T, Truchet B, Webber M, Wills T, et al. LTP but not seizure is associated with up-regulation of AKAP-150. Eur J Neurosci. 2003; 17:331–340. [PubMed: 12542670]

Gil OD, Needleman L, Huntley GW. Developmental patterns of cadherin expression and localization in relation to compartmentalized thalamocortical terminations in rat barrel cortex. J Comp Neurol. 2002; 453:372–388. [PubMed: 12389209]

Gorski JA, Gomez LL, Scott JD, Dell'Acqua ML. Association of an A-kinase-anchoring protein signaling scaffold with cadherin adhesion molecules in neurons and epithelial cells. Mol Biol Cell. 2005; 16:3574–3590. [PubMed: 15930126]

Haber M, Zhou L, Murai KK. Cooperative astrocyte and dendritic spine dynamics at hippocampal excitatory synapses. J Neurosci. 2006; 26:8881–8891. [PubMed: 16943543]

Huntley GW. Dynamic aspects of cadherin-mediated adhesion in synapse development and plasticity. Biol Cell. 2002; 94:335–344. [PubMed: 12500941]

Huntley GW, Benson DL. Neural (N)-cadherin at developing thalamocortical synapses provides an adhesion mechanism for the formation of somatopically organized connections. J Comp Neurol. 1999; 407:453–471. [PubMed: 10235639]

Husi H, Ward MA, Choudhary JS, Blackstock WP, Grant SG. Proteomic analysis of NMDA receptor-adhesion protein signaling complexes. Nat Neurosci. 2000; 3:661–669. [PubMed: 10862698]

Ito K, Okamoto I, Araki N, Kawano Y, Nakao M, Fujiyama S, Tomita K, Mimori T, Saya H. Calcium influx triggers the sequential proteolysis of extracellular and cytoplasmic domains of E-cadherin, leading to loss of beta-catenin from cell-cell contacts. Oncogene. 1999; 18:7080–7090. [PubMed: 10597309]

Jontes JD, Emond MR, Smith SJ. In vivo trafficking and targeting of N-cadherin to nascent presynaptic terminals. J Neurosci. 2004; 24:9027–9034. [PubMed: 15483121]

Juliano RL. Signal transduction by cell adhesion receptors and the cytoskeleton: functions of integrins, cadherins, selectins, and immunoglobulin-superfamily members. Annu Rev Pharmacol Toxicol. 2002; 42:283–323. [PubMed: 11807174]

Jungling K, Eulenburg V, Moore R, Kemler R, Lessmann V, Gottmann K. N-cadherin transsynaptically regulates short-term plasticity at glutamatergic synapses in embryonic stem cell-derived neurons. J Neurosci. 2006; 26:6968–6978. [PubMed: 16807326]

Kaneko T, Fujiyama F, Hioki H. Immunohistochemical localization of candidates for vesicular glutamate transporters in the rat brain. J Comp Neurol. 2002; 444:39–62. [PubMed: 11835181]

Kido M, Obata S, Tanihara H, Rochelle JM, Seldin MF, Taketani S, Suzuki ST. Molecular properties and chromosomal location of cadherin-8. Genomics. 1998; 48:186–194. [PubMed: 9521872]

Kirov SA, Sorra KE, Harris KM. Slices have more synapses than perfusion-fixed hippocampus from both young and mature rats. J Neurosci. 1999; 19:2876–2886. [PubMed: 10191305]

Korematsu K, Redies C. Expression of cadherin-8 mRNA in the developing mouse central nervous system. J Comp Neurol. 1997; 387:291–306. [PubMed: 9336230]

Levy WB, Steward O. Synapses as associative memory elements in the hippocampal formation. Brain Res. 1979; 175:233–245. [PubMed: 487154]

Malenka RC, Nicoll RA. Long-term potentiation--a decade of progress? Science. 1999; 285:1870–1874. [PubMed: 10489359]

Manabe T, Togashi H, Uchida N, Suzuki SC, Hayakawa Y, Yamamoto M, Yoda H, Miyakawa T, Takeichi M, Chisaka O. Loss of cadherin-11 adhesion receptor enhances plastic changes in hippocampal synapses and modifies behavioral responses. Mol Cell Neurosci. 2000; 15:534–546. [PubMed: 10860580]

Marambaud P, Shioi J, Serban G, Georgakopoulos A, Sarner S, Nagy V, Baki L, Wen P, Efthimiopoulos S, Shao Z, et al. A presenilin-1/gamma-secretase cleavage releases the E-cadherin

intracellular domain and regulates disassembly of adherens junctions. Embo J. 2002; 21:1948–1956. [PubMed: 11953314]

Marrs GS, Theisen CS, Bruses JL. N-cadherin modulates voltage activated calcium influx via RhoA, p120-catenin, and myosin-actin interaction. Mol Cell Neurosci. 2009; 40:390–400. [PubMed: 19162191]

Mayford M, Barzilai A, Keller F, Schacher S, Kandel ER. Modulation of an NCAM-related adhesion molecule with long-term synaptic plasticity in Aplysia. Science. 1992; 256:638–644. [PubMed: 1585176]

Mendez P, De Roo M, Poglia L, Klauser P, Muller D. N-cadherin mediates plasticity-induced long-term spine stability. J Cell Biol. 2010; 189:589–600. [PubMed: 20440002]

Miskevich F, Zhu Y, Ranscht B, Sanes JR. Expression of multiple cadherins and catenins in the chick optic tectum. Mol Cell Neurosci. 1998; 12:240–255. [PubMed: 9828089]

Moga DE, Calhoun ME, Chowdhury A, Worley P, Morrison JH, Shapiro ML. Activity-regulated cytoskeletal-associated protein is localized to recently activated excitatory synapses. Neuroscience. 2004; 125:7–11. [PubMed: 15051140]

Monea S, Jordan BA, Srivastava S, DeSouza S, Ziff EB. Membrane localization of membrane type 5 matrix metalloproteinase by AMPA receptor binding protein and cleavage of cadherins. J Neurosci. 2006; 26:2300–2312. [PubMed: 16495457]

Murase S, Mosser E, Schuman EM. Depolarization drives beta-Catenin into neuronal spines promoting changes in synaptic structure and function. Neuron. 2002; 35:91–105. [PubMed: 12123611]

Mysore SP, Tai CY, Schuman EM. Effects of N-cadherin disruption on spine morphological dynamics. Front Cell Neurosci. 2007; 1:1–14. [PubMed: 18946519]

Nagy V, Bozdagi O, Huntley GW. The extracellular protease matrix metalloproteinase-9 is activated by inhibitory avoidance learning and required for long-term memory. Learn Mem. 2007; 14:655–664. [PubMed: 17909100]

Nagy V, Bozdagi O, Matynia A, Balcerzyk M, Okulski P, Dzwonek J, Costa RM, Silva AJ, Kaczmarek L, Huntley GW. Matrix metalloproteinase-9 is required for hippocampal late-phase long-term potentiation and memory. J Neurosci. 2006; 26:1923–1934. [PubMed: 16481424]

Navone F, Jahn R, di Gioia G, Stukenbrok H, Greengard P, De Camilli P. Protein p38: an integral membrane protein specific for small vesicles of neurons and neuroendocrine cells. J Cell Biol. 1986; 103:2511–2527. [PubMed: 3097029]

Nuriya M, Huganir RL. Regulation of AMPA receptor trafficking by N-cadherin. J Neurochem. 2006; 97:652–661. [PubMed: 16515543]

Okamura K, Tanaka H, Yagita Y, Saeki Y, Taguchi A, Hiraoka Y, Zeng LH, Colman DR, Miki N. Cadherin activity is required for activity-induced spine remodeling. J Cell Biol. 2004; 167:961–972. [PubMed: 15569714]

Patel SD, Ciatto C, Chen CP, Bahna F, Rajebhosale M, Arkus N, Schieren I, Jessell TM, Honig B, Price SR, et al. Type II cadherin ectodomain structures: implications for classical cadherin specificity. Cell. 2006; 124:1255–1268. [PubMed: 16564015]

Popov VI, Davies HA, Rogachevsky VV, Patrushev IV, Errington ML, Gabbott PL, Bliss TV, Stewart MG. Remodelling of synaptic morphology but unchanged synaptic density during late phase long-term potentiation (LTP): a serial section electron micrograph study in the dentate gyrus in the anaesthetised rat. Neuroscience. 2004; 128:251–262. [PubMed: 15350638]

Redies C, Takeichi M. Expression of N-cadherin mRNA during development of the mouse brain. Dev Dyn. 1993; 197:26–39. [PubMed: 8400409]

Rhee J, Mahfooz NS, Arregui C, Lilien J, Balsamo J, VanBerkum MF. Activation of the repulsive receptor Roundabout inhibits N-cadherin-mediated cell adhesion. Nat Cell Biol. 2002; 4:798–805. [PubMed: 12360290]

Saglietti L, Dequidt C, Kamieniarz K, Rousset MC, Valnegri P, Thoumine O, Beretta F, Fagni L, Choquet D, Sala C, et al. Extracellular interactions between GluR2 and N-cadherin in spine regulation. Neuron. 2007; 54:461–477. [PubMed: 17481398]

Seto A, Hasegawa M, Uchiyama N, Yamashima T, Yamashita J. Alteration of E-cadherin and alpha N-catenin immunoreactivity in the mouse spinal cord following peripheral axotomy. J Neuropathol Exp Neurol. 1997; 56:1182–1190. [PubMed: 9370228]

Silverman JB, Restituito S, Lu W, Lee-Edwards L, Khatri L, Ziff EB. Synaptic anchorage of AMPA receptors by cadherins through neural plakophilin-related arm protein AMPA receptor-binding protein complexes. J Neurosci. 2007; 27:8505–8516. [PubMed: 17687028]

Smith TD, Adams MM, Gallagher M, Morrison JH, Rapp PR. Circuit-specific alterations in hippocampal synaptophysin immunoreactivity predict spatial learning impairment in aged rats. J Neurosci. 2000; 20:6587–6593. [PubMed: 10964964]

Sorra KE, Harris KM. Stability in synapse number and size at 2 hr after long-term potentiation in hippocampal area CA1. J Neurosci. 1998; 18:658–671. [PubMed: 9425008]

Steward O. Topographic organization of the projections from the entorhinal area to the hippocampal formation of the rat. J Comp Neurol. 1976; 167:285–314. [PubMed: 1270625]

Steward O, Halpain S. Lamina-specific synaptic activation causes domain- specific alterations in dendritic immunostaining for MAP2 and CAM kinase II. J Neurosci. 1999; 19:7834–7845. [PubMed: 10479686]

Steward O, Tomasulo R, Levy WB. Blockade of inhibition in a pathway with dual excitatory and inhibitory action unmasks a capability for LTP that is otherwise not expressed. Brain Res. 1990; 516:292–300. [PubMed: 2364294]

Steward O, Wallace CS, Lyford GL, Worley PF. Synaptic activation causes the mRNA for the IEG Arc to localize selectively near activated postsynaptic sites on dendrites. Neuron. 1998; 21:741–751. [PubMed: 9808461]

Stewart MG, Harrison E, Rusakov DA, Richter-Levin G, Maroun M. Re-structuring of synapses 24 hours after induction of long-term potentiation in the dentate gyrus of the rat hippocampus in vivo. Neuroscience. 2000; 100:221–227. [PubMed: 11008162]

Suzuki SC, Furue H, Koga K, Jiang N, Nohmi M, Shimazaki Y, Katoh-Fukui Y, Yokoyama M, Yoshimura M, Takeichi M. Cadherin-8 is required for the first relay synapses to receive functional inputs from primary sensory afferents for cold sensation. J Neurosci. 2007; 27:3466–3476. [PubMed: 17392463]

Tai CY, Mysore SP, Chiu C, Schuman EM. Activity-regulated N-cadherin endocytosis. Neuron. 2007; 54:771–785. [PubMed: 17553425]

Takeichi M. Cadherins: a molecular family important in selective cell-cell adhesion. Annu Rev Biochem. 1990; 59:237–252. [PubMed: 2197976]

Tamura K, Shan WS, Hendrickson WA, Colman DR, Shapiro L. Structure-function analysis of cell adhesion by neural (N-) cadherin. Neuron. 1998; 20:1153–1163. [PubMed: 9655503]

Tanaka H, Shan W, Phillips GR, Arndt K, Bozdagi O, Shapiro L, Huntley GW, Benson DL, Colman DR. Molecular modification of N-cadherin in response to synaptic activity. Neuron. 2000; 25:93–107. [PubMed: 10707975]

Tanaka Y, Nakanishi H, Kakunaga S, Okabe N, Kawakatsu T, Shimizu K, Takai Y. Role of nectin in formation of E-cadherin-based adherens junctions in keratinocytes: analysis with the N-cadherin dominant negative mutant. Mol Biol Cell. 2003; 14:1597–1609. [PubMed: 12686612]

Tang L, Hung CP, Schuman EM. A role for the cadherin family of cell adhesion molecules in hippocampal long-term potentiation. Neuron. 1998; 20:1165–1175. [PubMed: 9655504]

Tian L, Stefanidakis M, Ning L, Van Lint P, Nyman-Huttunen H, Libert C, Itohara S, Mishina M, Rauvala H, Gahmberg CG. Activation of NMDA receptors promotes dendritic spine development through MMP-mediated ICAM-5 cleavage. J Cell Biol. 2007; 178:687–700. [PubMed: 17682049]

Togashi H, Abe K, Mizoguchi A, Takaoka K, Chisaka O, Takeichi M. Cadherin regulates dendritic spine morphogenesis. Neuron. 2002; 35:77–89. [PubMed: 12123610]

Toni N, Buchs PA, Nikonenko I, Bron CR, Muller D. LTP promotes formation of multiple spine synapses between a single axon terminal and a dendrite. Nature. 1999; 402:421–425. [PubMed: 10586883]

Uchida N, Honjo Y, Johnson KR, Wheelock MJ, Takeichi M. The catenin/cadherin adhesion system is localized in synaptic junctions bordering transmitter release zones. J Cell Biol. 1996; 135:767–779. [PubMed: 8909549]

van Lookeren Campagne M, Oestreicher AB, van der Krift TP, Gispen WH, Verkleij AJ. Freeze-substitution and Lowicryl HM20 embedding of fixed rat brain: suitability for immungold

ultrastructural localization of neural antigens. J Histochem Cytochem. 1991; 39:1267–1279. [PubMed: 1833448]

Wang XB, Bozdagi O, Nikitczuk JS, Zhai ZW, Zhou Q, Huntley GW. Extracellular proteolysis by matrix metalloproteinase-9 drives dendritic spine enlargement and long-term potentiation coordinately. Proc Natl Acad Sci U S A. 2008; 105:19520–19525. [PubMed: 19047646]

Weeks AC, Ivanco TL, Leboutillier JC, Marrone DF, Racine RJ, Petit TL. Unique changes in synaptic morphology following tetanization under pharmacological blockade. Synapse. 2003; 47:77–86. [PubMed: 12422376]

Weeks AC, Ivanco TL, Leboutillier JC, Racine RJ, Petit TL. Sequential changes in the synaptic structural profile following long-term potentiation in the rat dentate gyrus: I. The intermediate maintenance phase. Synapse. 1999; 31:97–107. [PubMed: 10024006]

Weeks AC, Ivanco TL, Leboutillier JC, Racine RJ, Petit TL. Sequential changes in the synaptic structural profile following long-term potentiation in the rat dentate gyrus. II. Induction/early maintenance phase. Synapse. 2000; 36:286–296. [PubMed: 10819906]

Weeks AC, Ivanco TL, Leboutillier JC, Racine RJ, Petit TL. Sequential changes in the synaptic structural profile following long-term potentiation in the rat dentate gyrus: III. Long-term maintenance phase. Synapse. 2001; 40:74–84. [PubMed: 11170224]

Whitlock JR, Heynen AJ, Shuler MG, Bear MF. Learning induces long-term potentiation in the hippocampus. Science. 2006; 313:1093–1097. [PubMed: 16931756]

Wöhrn JC, Nakagawa S, Ast M, Takeichi M, Redies C. Combinatorial expression of cadherins in the tectum and the sorting of neurites in the tectofugal pathways of the chicken embryo. Neuroscience. 1999; 90:985–1000. [PubMed: 10218798]

Xie Z, Photowala H, Cahill ME, Srivastava DP, Woolfrey KM, Shum CY, Huganir RL, Penzes P. Coordination of synaptic adhesion with dendritic spine remodeling by AF-6 and kalirin-7. J Neurosci. 2008; 28:6079–6091. [PubMed: 18550750]

Yamagata M, Herman JP, Sanes JR. Lamina-specific expression of adhesion molecules in developing chick optic tectum. J Neurosci. 1995; 15:4556–4571. [PubMed: 7790923]

Yuste R, Bonhoeffer T. Morphological changes in dendritic spines associated with long-term synaptic plasticity. Annu Rev Neurosci. 2001; 24:1071–1089. [PubMed: 11520928]

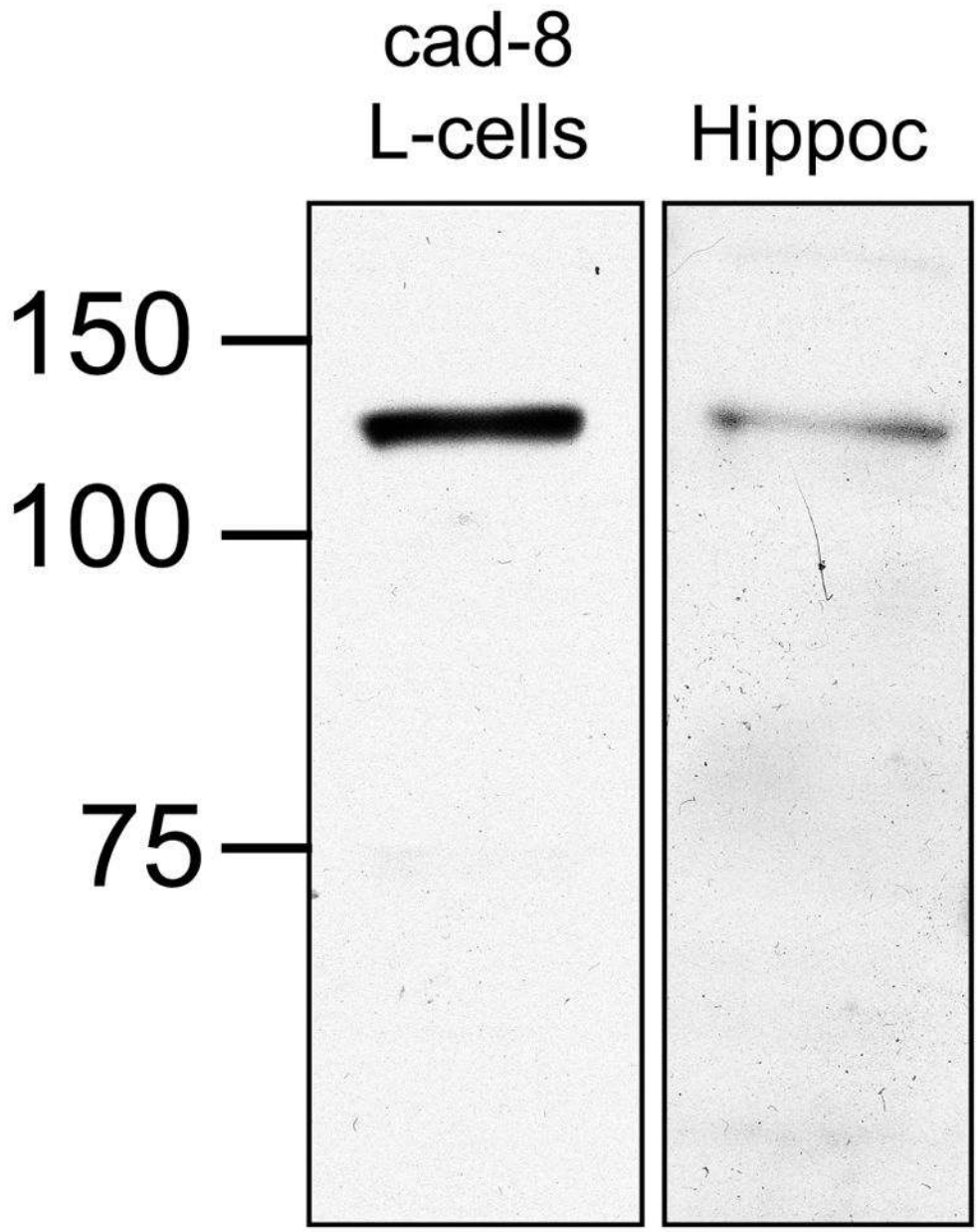

Fig. 1.
Immunoblot analysis verifying specificity of the cadherin-8 antiserum. A single band of the expected molecular mass was observed after blotting lysates prepared from L-cells transfected with full-length rat cadherin-8 (left) or from whole adult hippocampus (right).

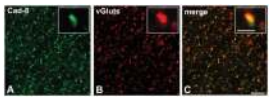

Fig. 2.

Cadherin-8 is synaptic. High-resolution confocal microscope images through the MML of dentate gyrus from an unstimulated adult rat immunofluorescently labeled for cadherin-8 (**A,** cad-8) or for the presynaptic terminal marker vGluts (**B**), shown separately and in a merged image (**C**), where regions of yellow indicate codistribution of cadherin-8 and vGluts (insets). Bars = 5 μm or 1.5 μm (insets).

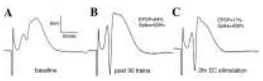

Fig. 3.

Representative example of HFS-induced LTP in dentate gyrus *in vivo*. The traces illustrate perforant path evoked responses before stimulation (**A**, baseline), after 3 X 10, 400Hz trains (**B**, the standard LTP induction paradigm) and after 2hrs of repeated stimulation (**C**, one 400Hz train/10secs). The percent increase in EPSP slope and population spike amplitude after the standard LTP induction paradigm and after 2 hrs of repeated stimulation are shown for comparison. These traces illustrate a phenomenon that is typically seen with prolonged stimulation: the slope of the EPSP decreases and there is an overall decrease in the amplitude of the late positive response.

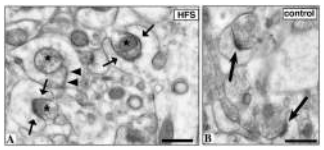

Fig. 4.

Synaptic structural remodeling with HFS *in vivo*. Representative electron micrographs of the dentate gyrus MML taken from a rat receiving LTP-inducing HFS (**A**) or one receiving non-potentiating control stimulation (**B**). Short arrows (A) show examples of significant morphological changes to dendritic spines ("concave" synapses) with HFS as expected. Spines enwrap the presynaptic terminals (asterisks), and sometimes form novel membrane appositions (arrowheads). In contrast, with control stimulation (B), synapses appear more conventional (arrows) with little or no concavity. Bars = 500 nm.

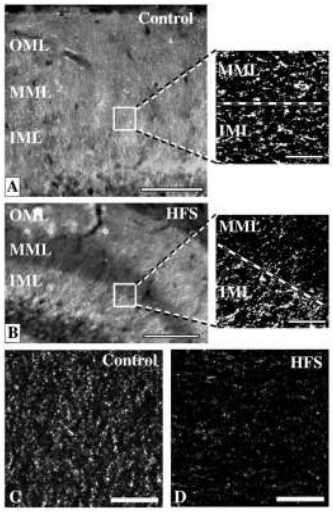

Fig. 5.

Loss of cadherin-8 immunolabeling in the MML with HFS. Representative confocal microscope images of cadherin-8 immunofluorescent labeling in the dentate gyrus molecular layer from a rat receiving control stimulation (**A, C**) or one receiving HFS (1 hr) (**B, D**). In control conditions (A), cadherin-8 is homogeneously distributed across the molecular layer. The higher-power inset (A) shows a uniform distribution of cadherin-8 puncta across the border that separates the IML from the MML (dotted line); within the MML under control conditions (C), dense immunofluorescent puncta are evident. With HFS (B), a dark band of greatly diminished cadherin-8 immunolabeling is present in the MML, flanked by normal-appearing bands of immunolabel corresponding to the IML and OML; the higher-power images (inset and D) shows diminished cadherin-8 immunolabeling in the MML. Abbreviations in this and subsequent figures: OML, outer molecular layer; MML, middle molecular layer; IML, inner molecular layer. Bar in A, B = 200 μm (A, B insets = 10 μm); Bar in C, D = 100 μm.

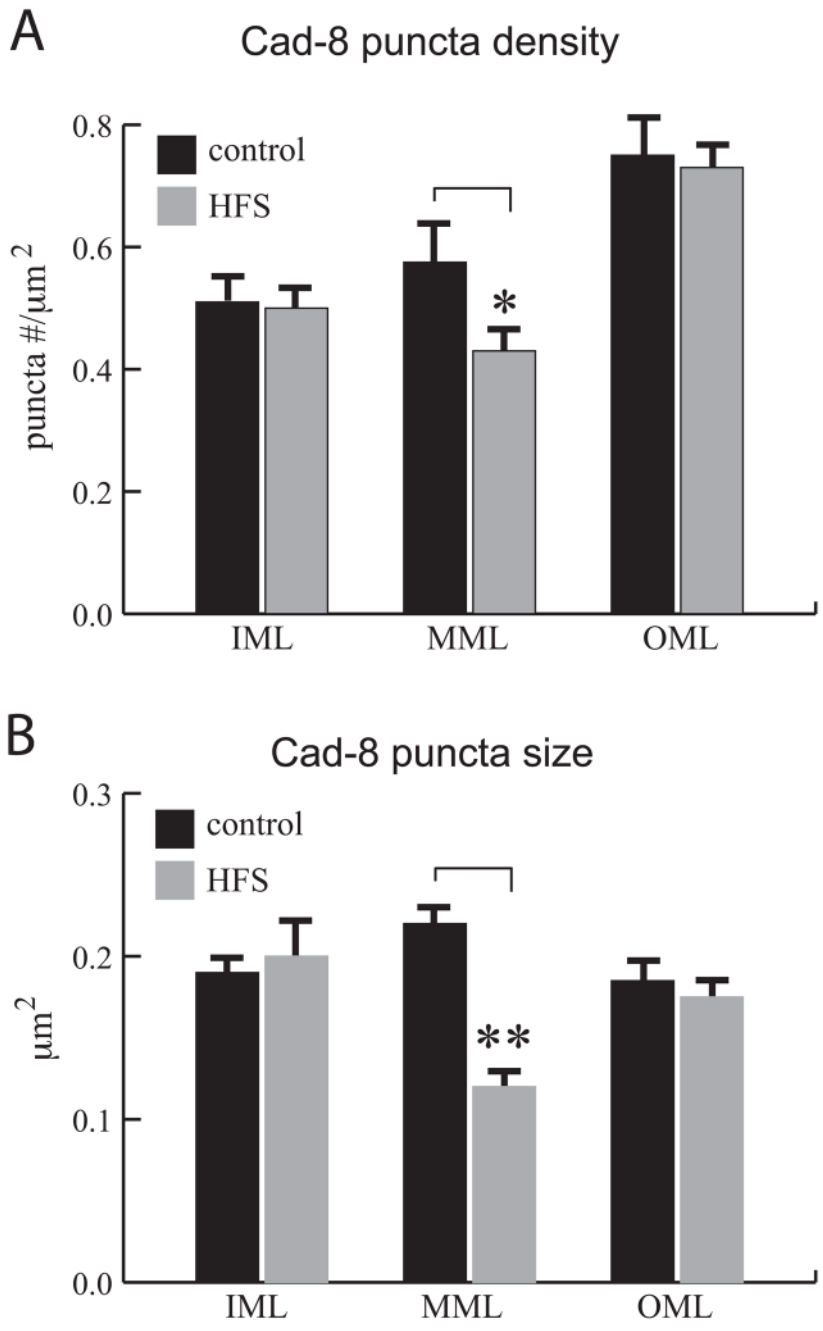

Fig. 6.

Quantification of density and size of cadherin-8 puncta in dentate gyrus molecular layer following HFS. The mean density (**A**) and sizes (**B**) of cadherin-8 (cad-8) puncta are significantly diminished in the MML of HFS rats in comparison with rats receiving control stimulation. *p<0.01 or **p<0.0001. There are no significant differences between conditions in density or size of cadherin-8 puncta in non-stimulated, flanking layers. n = 4 LTP rats and 3 control rats.

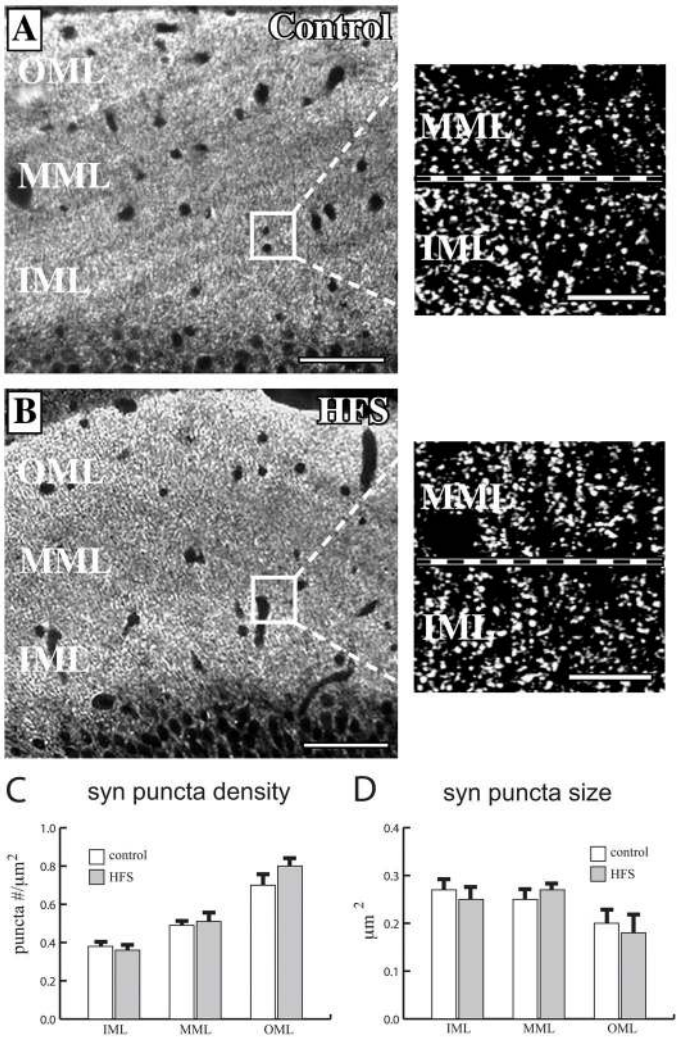

Fig. 7.

Synaptophysin labeling in dentate gyrus molecular layer is unchanged by HFS. Representative confocal microscope images of synaptophysin immunofluorescent labeling in the dentate gyrus molecular layer taken from the same animals shown in Fig. 5. The pattern of synaptophysin immunolabeling in rats receiving control stimulation (**A**) is similar to that in rats receiving HFS (**B**), with no apparent differences in density across the border that separates the IML from the MML (dotted lines, insets). The qualitative impressions were confirmed quantitatively; there were no significant differences between stimulation conditions in density (**C**) or sizes (**D**) of synaptophysin (syn) puncta in any layers. Bars = 200 μm (10 μm, insets); n = 4 LTP rats and 3 control rats.

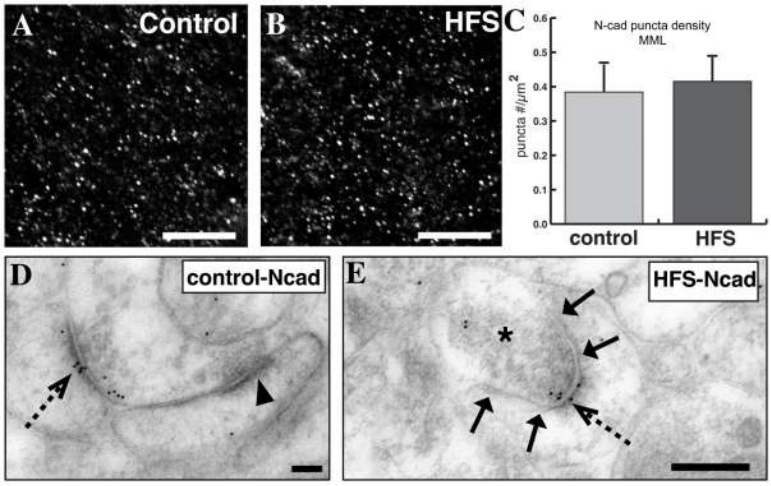

Fig. 8.

N-cadherin labeling is unchanged by HFS. Representative confocal microscope images (**A, B**) or electron-micrographs (**D, E**) showing N-cadherin localization in the MML of rat receiving control stimulation (A, D) or one receiving HFS (2 hrs) (B, E). Quantitatively, there were no differences between stimulation conditions in the density of N-cadherin (N-cad) immunofluorescent puncta in the MML (C). Post-embedding immunogold localization of N-cadherin at control synapses (D) shows typical clustering of gold-particles at apposed pre- and postsynaptic membranes (open arrow), with some synapses unlabeled (arrowhead). In the HFS rats (E), N-cadherin gold clustering was still evident (open arrows) at remodeled (concave) synapses where spines (arrows) wrap around presynaptic terminals (asterisk). Bars = 100 μm (A, B), 100 nm (D), or 250 nm (E).